IL NUOVO CIMENTO Vol. 27 C, N. 3 Maggio-Giugno 2004
DOI 10.1393/ncc/i2004-10008-0

A simple snowmelt parameterization for an Arctic site(*)

M. Nardino(**) and T. Georgiadis
IBIMET-CNR, Sezione di Bologna - Via Gobetti 101, I-40129 Bologna, Italy

(ricevuto il 15 Aprile 2004; revisionato l'1 Ottobre 2004; approvato il 5 Novembre 2004)

Summary. — Daily snow melt rates and corresponding changes in snow depth were determined through micrometeorological measurements of surface radiation and energy partition at Ny-Ålesund (Svalbard Islands) during a short experimental campaign. The daily rates computed using micrometeorological techniques closely match direct measurements of snow depths with a mean error of about 6%. The present findings are relevant in Polar areas because of the extreme susceptibility of the local environment to sudden changes of surface properties, namely as regards to the regulation of the sea ice- atmosphere-ocean system and surface biological activity. The simple parameterizations utilized are suitable to model the short-time melting process.

PACS 92.40.Rm – Snow.
PACS 92.60.Ry – Climatology.
PACS 92.70.Ly – Water cycles.

1. – Introduction

The high albedo and low thermal conductivity of snow cover over land are fundamental in the regulation of the Earth's radiation balance, which is the primary driving factor of the global atmospheric circulation system [1, 2].

In the northern hemisphere the mean monthly fraction of continental land covered by snow ranges from 7% to 40% during the year, making snow cover the most rapidly varying large-scale surface feature of the Earth [3, 4]. Most of the snow-covered surface belongs to the Arctic where large extents of sea-ice crust can form and disappear in a very short time as a function of the surface energy balance.

During the warm seasons in the Arctic solar heating melts the upper layers of the ice sheet and of the snow cover releasing fresh meltwater over the surface. These areas of snowmelt have a temperature of 0°C and interact with the atmosphere, the ocean and

(*) The authors of this paper have agreed to not receive the proofs for correction.
(**) E-mail: M.Nardino@ibimet.cnr.it

the ice surfaces absorbing more solar radiation than the nearby surfaces thus leading to differential solar radiation partition [5].

An understanding of the influence of synoptic weather systems on local and microscale climatology is also crucial in the determination of the resulting melt rates of snowpacks [6-8]. Advection of heat from the boundaries, due to the movements of relatively warm and moist air masses, can originate melting processes because of the sensible heat flux extracted from the lower layers of the atmosphere and directed toward the surface [9]. The depth of the resulting cooled layer depends on the horizontal wind speed and on the presence of large vertical wind shear; turbulent mixing appears to be the mechanism that modifies the air mass.

On the other hand, radiative fluxes in the Polar regions are strongly modulated by the presence of clouds. Their effects on the surface energy budget are of particular importance because of the sensitivity of sea-ice thickness to surface irradiances [10]. In overcast conditions during the warm seasons long-wave radiation dominates the radiative energy budget increasing the occurrence of melting processes [11,12]. Snowmelt processes can thus be considered the result of both effects due to the surface absorption of radiation and turbulent transport [13].

Because of the paramount importance of the surface albedo in regulating the components of the climatic system, melting processes appear to have a key role in governing the global radiation balance. They also have effects on the water vapor content of the atmosphere, originating feed-back mechanisms between the surface and the cloud cover [14].

The aim of this study is to furnish a simple parameterization of snowmelt events because of the importance of this process strictly linked to climate variations and involving important effects on the local biota habits; snowmelt rates and resulting snow depth variations are computed from micrometeorological measurements at the Ny-Ålesund site while at the same time defining the relationships with the radiative and turbulent environment.

2. – Experimental set-up

The experimental campaign was conducted at the Ny-Ålesund Scientific Arctic Base (78° 55′ N, 11° 56′ E) in the Svalbard Islands, 7 May–30 June, 1999.

The following instrumentation was deployed at the experimental facility: a radiometric station (Kipp and Zonen, mod. CNR1) to determine the whole short- and long-wave radiative balance, a sonic anemometer (Metek, mod. USAT1) to define the characteristics of the surface-atmosphere interaction and determine the sensible heat flux through eddy-correlation techniques [15], and a heat flux plate to determine the subsurface heat flux.

The anemometric data were stored on a PC after the electronic processing conducted by a programmable internal board, which computes two axis rotations, 15 min averages of the main physical atmospheric quantities, standard deviations, along with the determination of the momentum and sensible heat fluxes. Radiation partition and subsurface data were acquired by means of a CR10 Campbell data logger and stored into a Campbell SM192 memory module every 15 min. The sonic anemometer and the radiometer were placed on a pole at 3.5 and 1.5 m above the ground, respectively. The flux plate was buried into the snow and successively, after total snowmelt, into the ground at a 5 cm depth.

The cloud cover index as well as other meteorological parameters utilized in the study were obtained by the close station of Alfred Wegener and Norwegian Polar Institutes.

3. – Method

Energy balance over a melting surface is given by [7]

$$R_{\mathrm{n}} = G + H_0 + LE + E_{\mathrm{m}} + E_{\mathrm{p}}\,, \tag{1}$$

where R_{n} is the net radiation, G the subsurface heat flux, H_0 and LE the sensible and latent heat fluxes, E_{m} the energy due to the surface melting, and E_{p} the precipitation heat flux.

The latent heat flux has been computed through the bulk formulation

$$LE = \frac{\rho u_*^2}{u}\lambda(q_0 - q_z)\,, \tag{2}$$

where ρ is the air density in kg m^{-3}, u_* the friction velocity in m s^{-1}, u the wind speed in m s^{-1}, λ the latent heat (equal to 2833 J g^{-1} in the case of sublimation and 2256 J g^{-1} for evaporation), q_0 the surface specific humidity in g kg^{-1}, and q_z the specific humidity at the measurement height z in g kg^{-1}. Measurements of specific humidity came from the Koldewey station (AWI/DMPI-NP) which is 100 meters away. In the computation of the latent heat flux the latent heat of vaporization was utilized because during the whole melting processes the surface air temperature was almost continuously over 0 °C corresponding to a maximum correlated error of about 12%.

The E_{p} term of eq. (1) can be ignored when precipitation events are negligible as in the case of the recorded measurements with the only exception of day 05/13/1999 where precipitation value reached about 20 mm [13].

To calculate the rate of snowmelt from the measured values the following equation applies [13]:

$$\begin{aligned} S_{\mathrm{m}}\mathrm{rate} = (R_{\mathrm{n}} - G)\cdot 10^{-6}\times 3600\times 2.99 - \Big[\rho C_p 10^{-3} K_{\mathrm{H}}\,(T_z - T_0)\,u + \\ +\rho\lambda K_{\mathrm{L}}\,(0.622/P_{\mathrm{a}})\,(e_{sz} - e_{s0})\,u\Big]\times 3600\times 2.99\,, \end{aligned} \tag{3}$$

where S_{m} is the rate of snow melting in mm h^{-1}, ρ the air density in kg m^{-3}, C_p the specific heat at constant pressure ($C_p = 1.01\cdot 10^{-3}$ MJ kg^{-1} K^{-1}), T_z the temperature at the measurement height in °C, T_0 the surface temperature in °C, u the wind speed, λ the latent heat of vaporization for water, P_{a} the air pressure in hPa, e_{sz} the vapor pressure at height z in hPa, e_{s0} the surface vapor pressure in hPa, and K_{H} and K_{L} the bulk transfer coefficients assumed equal to 0.0023 [15].

Since the data were taken every 3 h the multiplying factor of the two terms on the right-hand side of eq. (3) becomes $3600\times 3\times 2.99$.

The same equation was used to compute the daily values of the snowmelt rate: the measured terms are the daily mean values and the corresponding multiplying factor is $3600\times 24\times 2.99$.

Following the statistical approach of [13] the three hourly melt values were summed over periods of 24 h and then compared with daily mean values.

Finally, a comparison with measured values of the snow depth (taken by the Norwegian Meteorological Institute and the Norwegian Polar Institute, DNMI/NP) for the whole measurement period was done, calculating the snow depth from the snowmelt rate.

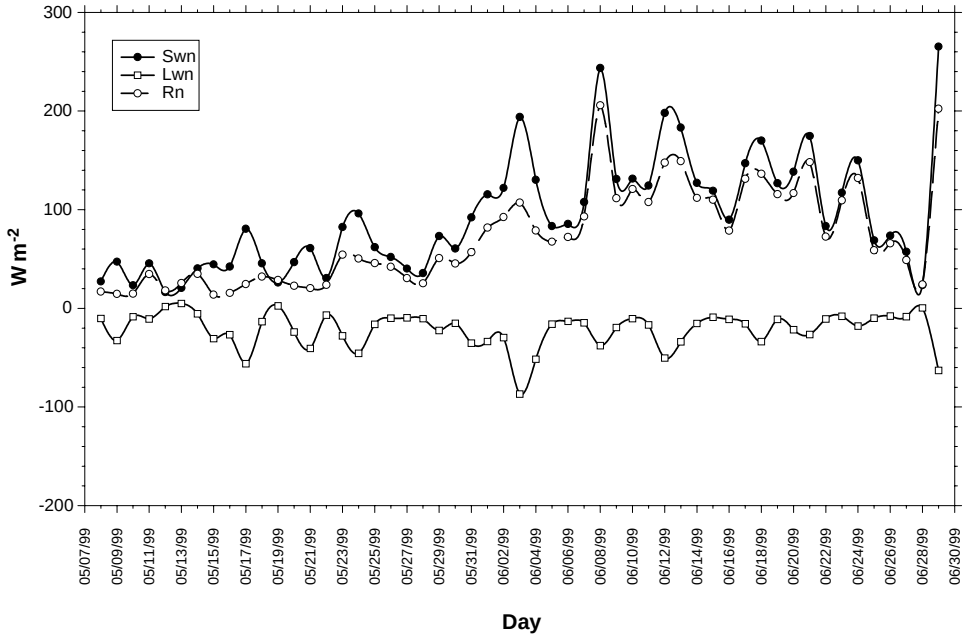

Fig. 1. – Daily mean values of surface radiative budget.

4. – Results and discussion

4˙1. *Characterization of melting period.* – Daily mean values of each measured quantity were computed to study the surface radiative balance.

Figure 1 illustrates the long- and short-wave daily mean balances, along with the net radiation that is positive for the entire period. Net radiation increases through the measurement period due to the increase of net short-wave radiation caused by changes in solar elevation angle.

The analysis of the daily mean of the single radiative components (fig. 2) indicates a slight increase in long-wave values, incoming and outgoing, and a sharp decrease in the short-wave components. Figure 3 shows the albedo trend, computed utilizing the ratio of the short-wave out and short-wave in components, which reflects the observed variations, due to surface optical properties modification, with an abrupt change during the period 5-9 June. During this time, the snow melted completely. The daily mean albedo values change from 0.8 at the beginning of the measurement period to about 0.5 during the first days of June, before dropping to 0.1 afterwards.

In fig. 4 the daily mean values of dry and wet air temperatures and wind speed for the whole measurement period are plotted. Note that the dry and wet temperatures during the period 15 May–3 June are normally below 0 °C. During this period three short melting episodes were recorded with corresponding temperatures higher than 0 °C and wind speeds ranging between 6 and 8 ms^{-1} which could indicate advections of warm air masses. The following days air temperature increases above 0 °C and the wind speed decreases, thus snowmelt can be attributed mainly to the temperature increase.

Figure 5 presents the daily mean value of the cloud cover index in tenths. Note that the melting occurs during cloudy days, as observed by [13] and [10].

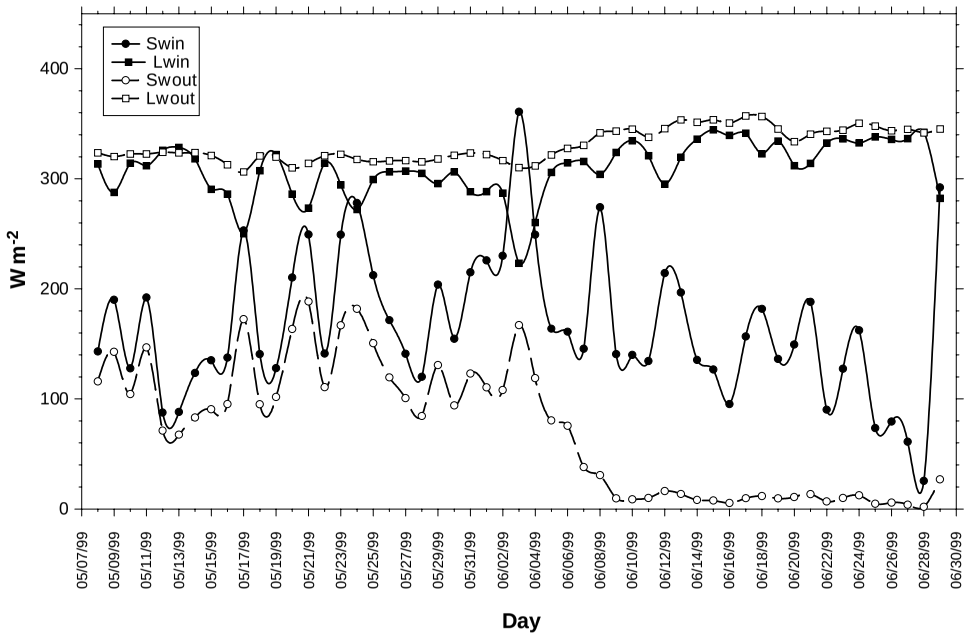

Fig. 2. – Daily mean values of radiative flux components.

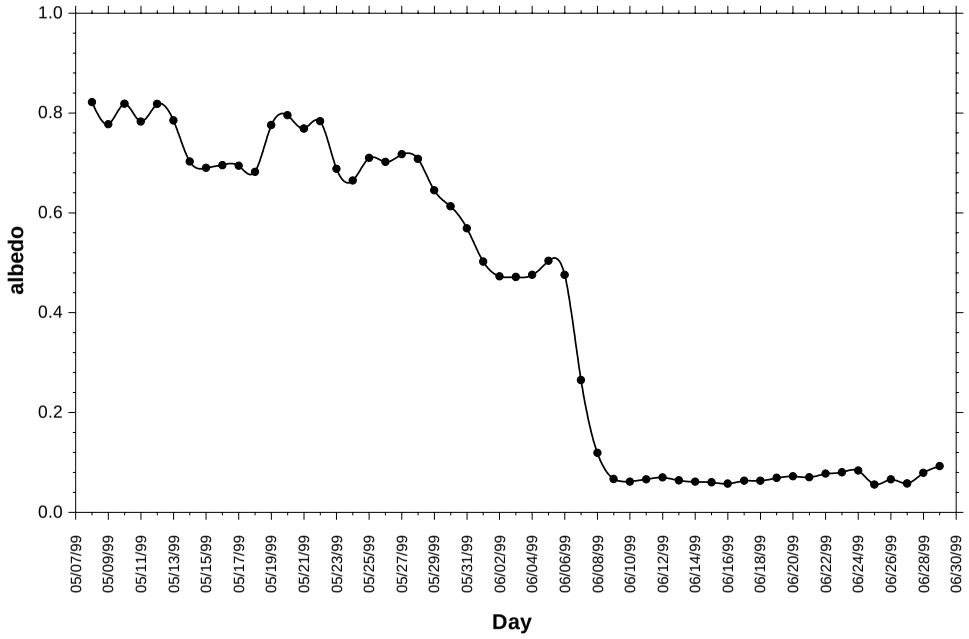

Fig. 3. – Daily mean values of surface albedo.

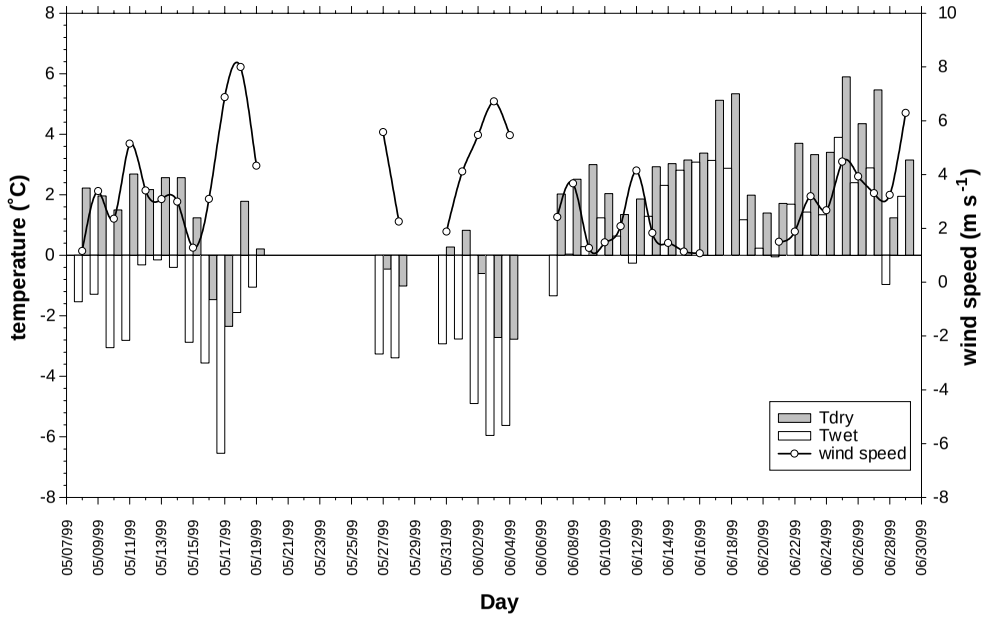

Fig. 4. – Daily mean values of dry and wet temperatures and wind speed.

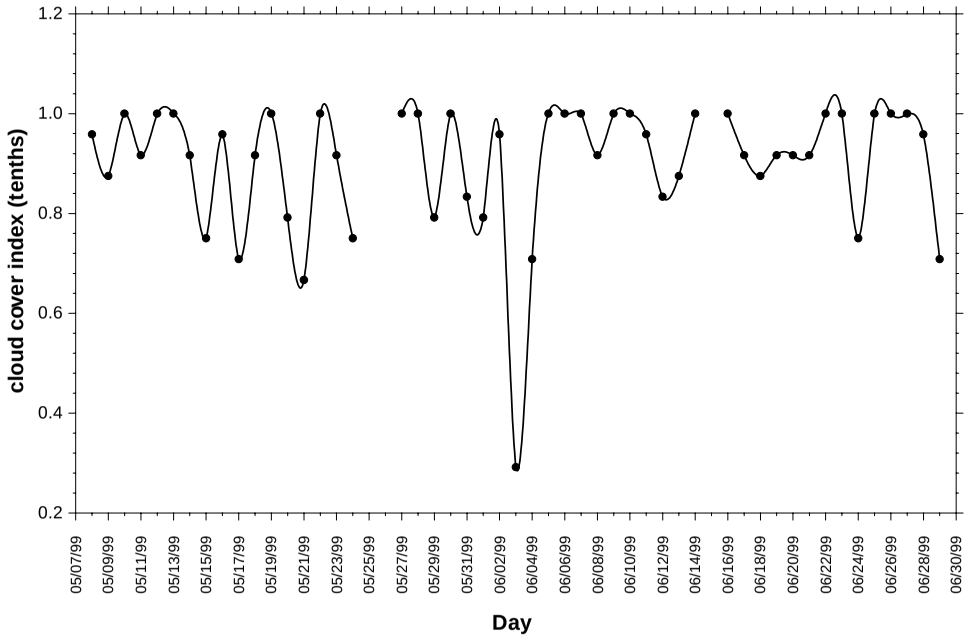

Fig. 5. – Daily mean values of cloud cover index.

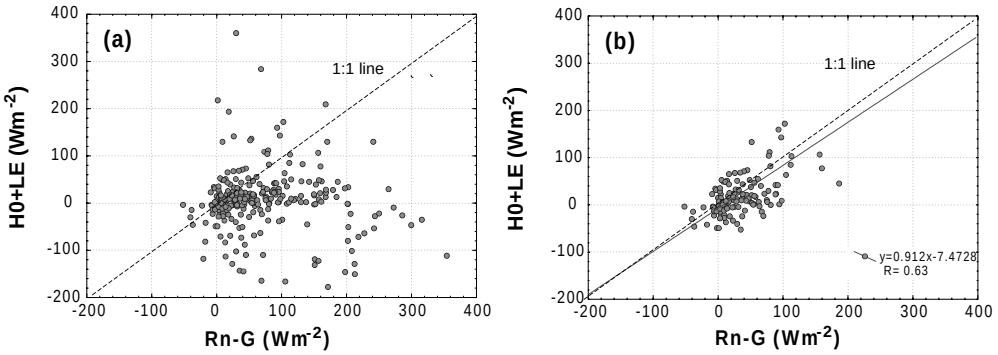

Fig. 6. – Scatter plots between the sum of sensible and latent heat fluxes *vs.* the difference between net radiation and subsurface heat flux for the 3-hour values considering a) all measurement days and b) without the intense melting period days (26 May–16 June).

In summary the melting event recorded at Ny-Ålesund during 1999 is characterized by cloudy, windy and low solar input conditions.

4˙2. *Surface energy balance*. – The surface energy balance has been computed through the radiometric and anemometric measurements and with the latent heat flux obtained with the bulk formula (2) using the humidity measurements at the Koldewey station.

The scatter plots between the sum of H_0 and LE and the difference of R_n and G are obtained considering all days of the campaign (fig. 6a) and eliminating those between 26 May and 16 June (fig. 6b) when the intense melting period was observed. Figure 6a illustrates that there is a missing energy component in the surface partition, attributable to different surface processes that we are not able to measure, and this reflects in a very low slope of the 1:1 scatter-plot.

If the surface energy balance is computed eliminating the period of intense melting (fig. 6b) the linear fit shows a good agreement with the surface energy balance and the slope of the regression line results very close to the 1:1 line even if a certain degree of scatter is obviously present.

The same analysis has been performed for the daily mean values and results are shown

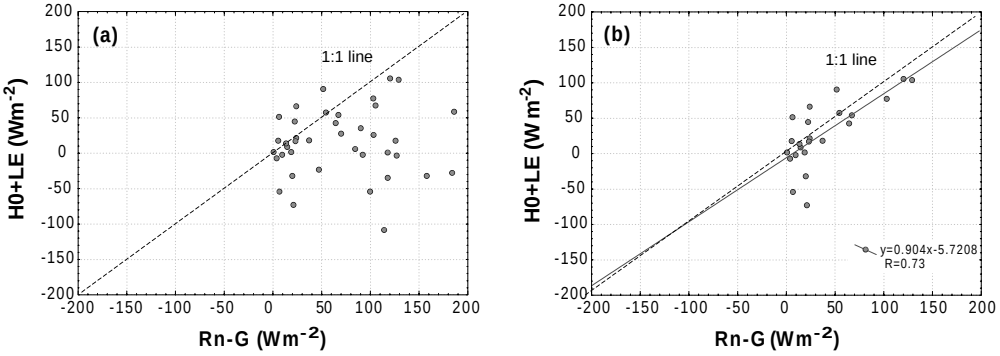

Fig. 7. – As in fig. 6 but for the daily mean values.

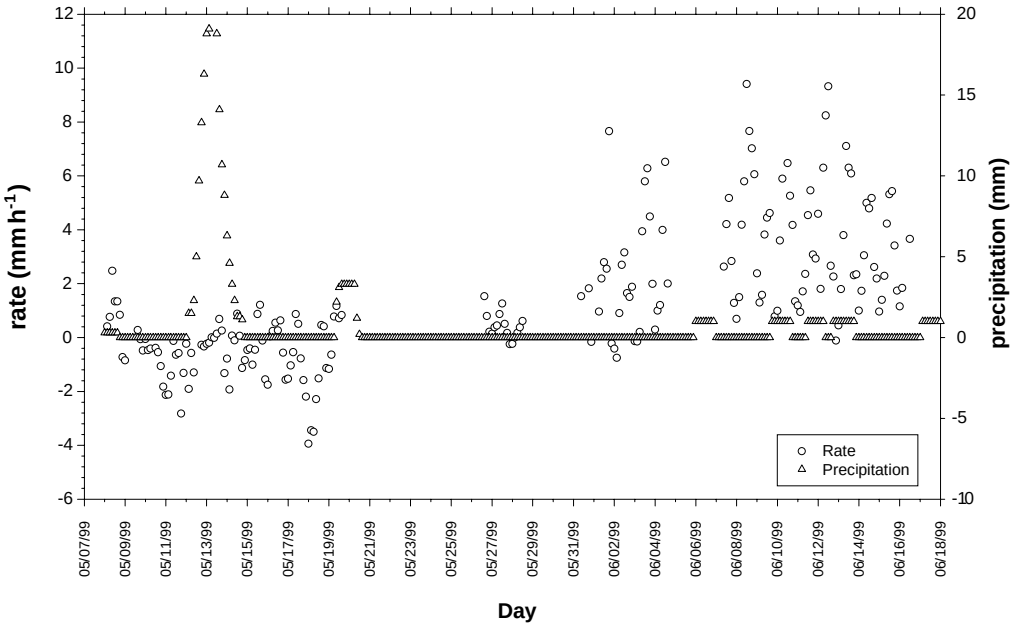

Fig. 8. – Time series of the snowmelt rate obtained with eq. (3) and precipitation measurements.

in fig. 7. As in the previous case, if all days are considered (fig. 7a) a strong deviation from the 1:1 line is present, whereas omitting the period between 26 May and 16 June (fig. 7b) results in a good agreement with the surface energy balance.

4˙3. *Computation of the snowmelt rate.* – In fig. 8 the snowmelt rates obtained with eq. (3) for the 3 h values are reported together with the precipitation values measured by DNMI/NP. The values are realistic because on average the snowmelt rate is about 4 mm every 3 h, which gives a realistic value of about 32 mm day^{-1} [13]. The negative values refer to a precipitation event as shown by the trend of the precipitation values.

Following the statistical methods of [13], daily melting rates have been computed adding eight of the 3-hourly values (fig. 9). On a daily basis the resulting melt rates, computed as the sum of different 3 h time periods, show a good agreement with a direct computation of the daily mean values. This finding implies that the statistics of melting rates, on a daily basis, are independent of the time step used for their computation, which disagrees with [13].

The daily snowmelt rates computed from micrometeorological measurements were used to calculate snow depths and successively compared with the measurements of DNMI/NP. The results are reported in fig. 10.

The snow depth was computed considering that

$$\frac{\partial h}{\partial t} = -\text{rate}$$

and

$$h = h_0 - \text{rate} \cdot t\,, \tag{4}$$

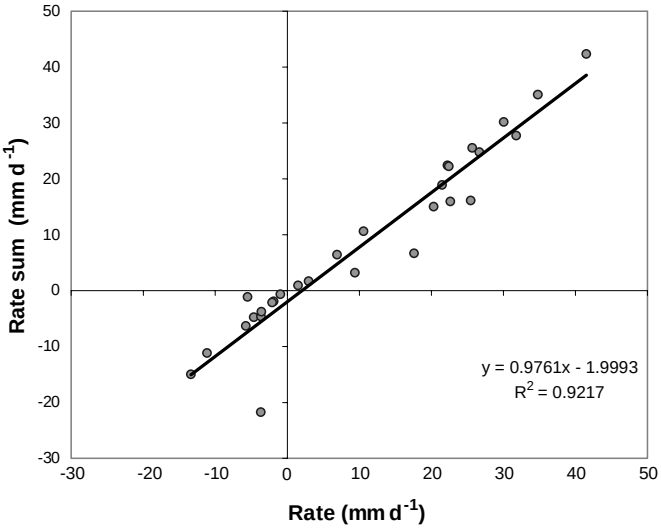

Fig. 9. – Scatter plot between the daily snowmelt rate obtained as a sum of the 3-hour values *vs.* the daily snowmelt rate obtained with the daily values in eq. (3).

where h is the snow depth, h_0 the initial snow depth, and t the time.

As an initial condition, h_0 was taken equal to the measured value and the computation was applied only when the intense melting period occurred (26 May–16 June).

Results show a very good agreement between the computed and measured values. Figure 10 shows the results for the daily mean values and the correlation coefficient is

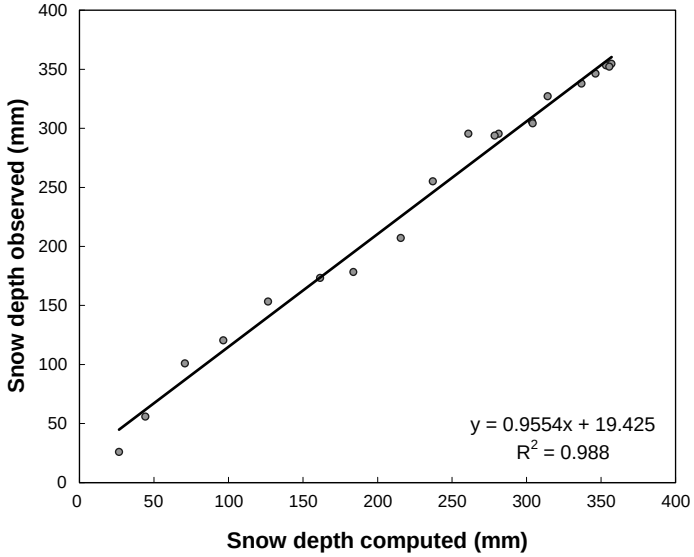

Fig. 10. – Scatter plot between the snow depth measured by DNMI/NP *vs.* the snow depth computed with eq. (4).

very high. The calculation overestimates snow depth by about 19 mm corresponding to a mean error of about 6%.

5. – Conclusions

The results obtained by micrometeorological measurements show that melting processes represent one of the most important energy partition components at the snow surface. This process is mainly regulated by the advection of heat from the boundaries of the investigated area, cloud cover index and wind speed.

Snow depth calculated from micrometeorological parameters resulted in good agreement with the direct measurements. These kinds of measurements can be applied to routine estimations, which results in reduced field logistic compared to the direct measurements performed at snow-covered sites.

The statistics of snow melting rates performed on a 3-hourly and on a daily basis did not show relevant differences thus allowing the use of existing data-bases for climatological characterizations and comparisons between different sites.

The parameterizations utilized appear to furnish a very good description of the temporal evolution of the process but some attention should be paid for their application in long-time period observations because of the strong time-dependence of the optical and mechanical properties of the snow.

* * *

The Alfred Wegener Institute is acknowledged for the availability of Koldewey data and DNMI/NP for the snow data. Special thanks to R. Sparapani, manager of the Dirigibile Italia base for his continuous assistance during the preparation of the experiment. The authors also wish to thank for their assistance J. B. Orbaek and S. Claes of the Norwegian Polar Institute and R. Pirazzini of the Finnish Marine Institute.

REFERENCES

[1] Slater A. G., Pitman A. J. and Desborough C.E., *Int. J. Climatol.*, **18** (1998) 595.
[2] Liston G. E., *J. Appl. Meteorol.*, **38** (1999) 1474.
[3] Hall D. K., *Rev. Geophys.*, **26** (1988) 26.
[4] Marsh P., *Hydrol. Processes*, **13** (1999) 2117.
[5] Hodgkins R., *Hydrol. Processes*, **15** (2001) 441.
[6] Harding R. H. and Pomeroy J. W., *J. Climate*, **9** (1996) 2778.
[7] Neale S. M. and Fitzharris B. B., *Int. J. Climatol.*, **17** (1997) 1595.
[8] Woo Ming-Ko, Yang D. and Young K. L., *Hidrol. Processes*, **13** (1999) 1859.
[9] Shook K. and Gray M., *Hydrol. Processes*, **11** (1997) 1725.
[10] Zhang T., Stamnes K. and Bowling S. A., *J. Climate*, **9** (1996) 2110.
[11] Curry J. A., Schramm J. L. and Ebert E. E., *Meteorol. Atmos. Phys.*, **51** (1993) 197.
[12] Nardino M., Orsini A., Pirazzini R., Calzolari F., Georgiadis T. and Levizzani V., *Cloud radiative forcing and effects on local climate*, in *Proceedings of ECAC 2000, 3rd European Conference on Applied Climatology, Pisa, Italy, October 16-20, 2000.*
[13] Hough M. N. and Hollis D., *Meteorol. Appl.*, **5** (1997) 127.
[14] LAPP Land Arctic Physical Processes, Final Report, Contract n° ENV4-CT95-0093. (1999).
[15] Stull R. B., in *An Introduction to Boundary Layer Meteorology* (Kluwer Academic Publishers, Dordrecht, Netherlands) 1st ed., 1988.